

EUROPEAN ORGANIZATION FOR NUCLEAR RESEARCH (CERN)



CERN-PH-EP-2015-215

LHCb-PAPER-2015-030

Okttober 8, 2015

Measurement of the time-integrated CP asymmetry in $D^0 \rightarrow K_s^0 K_s^0$ decays

The LHCb collaboration[†]

Abstract

The time-integrated CP asymmetry in the decay $D^0 \rightarrow K_s^0 K_s^0$ is measured using 3 fb^{-1} of proton-proton collision data collected by the LHCb experiment at centre-of-mass energies of 7 and 8 TeV. The flavour of the D^0 meson is determined by use of the decay $D^{*+} \rightarrow D^0 \pi^+$ and its charge conjugate mode. The result is

$$\mathcal{A}_{CP} = -0.029 \pm 0.052 \pm 0.022 ,$$

where the first uncertainty is statistical and the second systematic. The result is consistent with Standard Model expectations and improves the uncertainty with respect to the only previous measurement of this quantity by more than a factor of three.

Accepted by JHEP

© CERN on behalf of the LHCb collaboration, license CC-BY-4.0.

[†]Authors are listed at the end of this paper.

1 Introduction

In the Standard Model, CP violation in charm decays is expected to be small and hence potentially sensitive to contributions from New Physics. Although measurements of the time-integrated CP asymmetry in D^0 decays to pairs of charged mesons showed hints of CP asymmetry at the level of 0.7%, the combined results are not yet conclusive [1–5]. Of particular interest, both for the search of New Physics and for the understanding of penguin contributions, are decays of D^0 mesons into a pair of neutral mesons, such as the decay $D^0 \rightarrow K_s^0 K_s^0$ [6, 7].¹ If the CP asymmetry in D^0 decays to charged mesons is confirmed and assuming moderate breaking of the SU(3) flavour symmetry, the CP asymmetry of this mode could be of $\mathcal{O}(1\%)$ or even larger [6]. From a more recent Standard Model based analysis of the contributing amplitudes, a 95% confidence level upper limit of 1.1% for direct CP violation in the decay $D^0 \rightarrow K_s^0 K_s^0$ has been derived [7]. The single previous measurement gave $A_{CP} = (23 \pm 19)\%$ [8].

Here, we present the first result from the LHCb collaboration on CP violation in the decay $D^0 \rightarrow K_s^0 K_s^0$. The measurement is based on D^0 mesons originating from $D^{*+} \rightarrow D^0 \pi^+$ decays, where the flavour of the D^0 meson can be inferred from the charge of the “slow” pion from the D^{*+} decay. Throughout this document, D^{*+} stands for $D^*(2010)^+$. As a control channel, the decay $D^0 \rightarrow K^- \pi^+$ is used to estimate production and detection asymmetries. The analysis uses 3 fb^{-1} of proton-proton collision data collected with the LHCb detector in 2011 and in 2012, at centre-of-mass energies of 7 TeV and 8 TeV, respectively.

2 Detector and simulation

The LHCb detector [9, 10] is a single-arm forward spectrometer covering the pseudorapidity range $2 < \eta < 5$, designed for the study of particles containing b or c quarks. The detector includes a high-precision tracking system consisting of a silicon-strip vertex detector surrounding the pp interaction region, a large-area silicon-strip detector located upstream of a dipole magnet with a bending power of about 4 Tm, and three stations of silicon-strip detectors and straw drift tubes placed downstream of the magnet. The tracking system provides a measurement of momentum, p , of charged particles with a relative uncertainty that varies from 0.5% at low momentum to 1.0% at 200 GeV.² The minimum distance of a track to a primary vertex (PV), the impact parameter, is measured with a resolution of $(15 + 29/p_T) \mu\text{m}$, where p_T is the component of the momentum transverse to the beam, in GeV. The polarity of the dipole magnet is reversed regularly throughout the data-taking period, which allows to determine and correct for charge asymmetries due to the detector geometry.

Different types of charged hadrons are distinguished using information from two ring-imaging Cherenkov detectors. Photons, electrons and hadrons are identified by a

¹The inclusion of charge-conjugate processes is implied throughout this article.

²We use natural units where $c = 1$.

Table 1: Definition of candidate categories.

Categories	Description
LL	both K_s^0 are of category long and <i>not</i> selected by the dedicated trigger
LD	one K_s^0 is long, the other one is downstream
DD	both K_s^0 are downstream
LLtrig	both K_s^0 are of category long and selected by the dedicated trigger

calorimeter system consisting of scintillating-pad and preshower detectors, an electromagnetic calorimeter and a hadronic calorimeter. Muons are identified by a system composed of alternating layers of iron and multiwire proportional chambers. The online event selection is performed by a trigger, which consists of a hardware stage, based on information from the calorimeter and muon systems, followed by a software stage, which applies a full event reconstruction.

In the simulation, pp collisions are generated using PYTHIA [11] with a specific LHCb configuration [12]. Decays of hadronic particles are described by EVTGEN [13], in which final state radiation is generated using PHOTOS [14]. The interaction of the generated particles with the detector, and its response, are implemented using the GEANT4 toolkit [15] as described in Ref. [16].

3 Selection

Signal decays are reconstructed in the decay mode $D^{*+} \rightarrow D^0\pi^+$ with $D^0 \rightarrow K_s^0K_s^0$ and $K_s^0 \rightarrow \pi^+\pi^-$ [17]. To collect as many $D^0 \rightarrow K_s^0K_s^0$ decays as possible, events from all available physics triggers are considered. Candidate events are accepted if the four pions assigned to the K_s^0 decays are sufficient to trigger the event or if the rest of the event, without the slow pion from the D^* decay, satisfies a trigger condition. Excluding the slow pion from the trigger decision minimises any bias on the CP asymmetry due to the trigger.

The $K_s^0 \rightarrow \pi^+\pi^-$ decays are reconstructed in two different categories: the first involves K_s^0 mesons that decay early enough for the daughter pions to be reconstructed in the vertex detector; the second contains K_s^0 mesons that decay later such that daughter track segments are only reconstructed in the tracking detectors downstream of the vertex detector. These categories are referred to as *long* (L) and *downstream* (D), respectively. The less abundant long category has better momentum and vertex resolution than the downstream category. As the final state contains two K_s^0 mesons, there are three possible combinations labeled LL, LD, and DD. A dedicated software trigger selection for the $D^0 \rightarrow K_s^0K_s^0$ decay was implemented in 2012. As this trigger only accepts signal candidates composed of two long K_s^0 , a fourth D^0 category, LLtrig, is defined where the dedicated trigger accepted the signal candidate. The four categories are listed in Table 1.

The decay vertex of the D^0 candidate is reconstructed from the pion trajectories,

constraining the K_s^0 mass to its known value [18] and the D^0 flight direction to point to a PV [17]. To reduce the contamination from the decay $D^0 \rightarrow K_s^0\pi^+\pi^-$, only candidates with significant decay times for both K_s^0 decays are accepted. This requirement has a signal efficiency of over 99 %. The D^0 candidate is combined with a pion to produce a D^* candidate. Fiducial cuts are applied on the kinematic properties of this slow pion to remove regions where the detection charge asymmetry is large. A cut on the invariant mass of the $K_s^0K_s^0$ system of ± 20 MeV around the known value of the D^0 mass is applied. The efficiency of this cut is 98 % in all categories, except for DD, where it is 94 %. Candidates are further selected by requiring the difference between the D^{*+} and D^0 candidate masses, $\Delta m \equiv m_{D^*} - m_{D^0}$, to be less than 155 MeV.

To further reduce combinatorial background a multivariate analysis (MVA) method [19,20] is used. It is based on a rule-based learner applying the methods of bagging [21] and instance weighting (see, *e.g.*, Refs. [22,23]). Separate samples have been used for training and testing, where simulated events have been used as signal proxy, while the background sample was a mixture of data from D^0 sidebands (the mass ranges 1764.84 – 1844.84 MeV and 1884.84 – 1964.84 MeV) and simulation. Kinematic quantities, decay time variables, geometric quantities, and fit quality variables are used as input to the MVA. The selection of variables and the training have been done separately for the different categories. For the MVA optimisation, the figure of merit $S/\sqrt{S+B}$ is used, where S is the expected number of signal candidates in the signal region defined by a ± 1.5 MeV window around the known Δm value [18], while B is the number of background candidates in the signal region. The optimal points have signal efficiencies of 95 %, 51 %, 47 %, and 37 %, and background retentions of 50 %, 0.33 %, 0.40 %, and 0.73 % for LLtrig, LL, LD, and DD, respectively. The large background retention for the LLtrig category is due to the fact that the dedicated trigger intrinsically has a much lower background level. The control channel $D^0 \rightarrow K^-\pi^+$ is selected by cuts on kinematic quantities, vertex quality variables, geometric quantities, and decay time variables. In addition, the same mass requirements and fiducial cuts on the slow pion are applied as in case of the signal channel. Due to the large number of control channel candidates, which is much larger than needed for this analysis, 1 % of candidates are accepted at random.

4 Asymmetry measurement

The CP asymmetry is obtained as

$$\mathcal{A}_{CP} = \frac{N^+ - N^-}{N^+ + N^-} \quad (1)$$

for each category, where N^+ (N^-) is the yield determined from a fit to the data for a positive (negative) charge of the slow pion.

The yields are determined from an extended unbinned maximum likelihood fit to the Δm distribution. In the fit model, the signal is described by a sum of three Gaussian functions, where the two narrower ones are required to have the same mean value. The

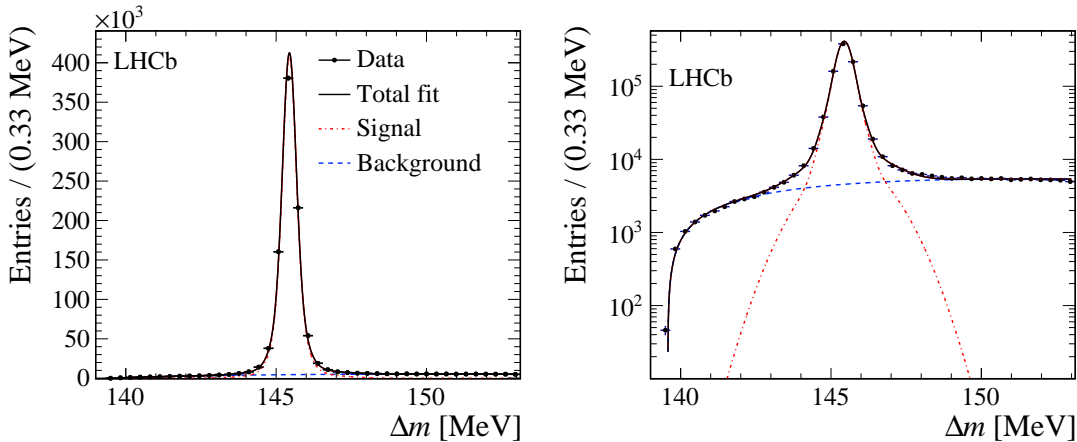


Figure 1: Distribution of Δm for the control channel $D^0 \rightarrow K^- \pi^+$ in (left) linear and in (right) logarithmic scale. The solid (black) line corresponds to the total fit, the dashed (blue) line corresponds to the background, and the dash-dotted (red) line represents the signal contribution.

parameters of the narrowest Gaussian function and the mean value of the widest one are allowed to float, while the ratios between widths, as well as those between normalisations, of all three are constrained to the values found in the simulation. The background is parametrised by the product of an exponential function and a power law for the phase-space threshold at the pion mass

$$f_{\text{bg}} = C_{\text{bg}} (\Delta m - m_{\pi^+})^p e^{-(\Delta m - m_{\pi^+})^\alpha}. \quad (2)$$

Here C_{bg} , p and α are determined by the fit. Independent fits are performed for the four categories. In each category, the background parameters and the shape parameters of the signal component are shared between the two charges of the slow pion.

The Δm distribution for the control channel, summed over both charges of the slow pion with the fit function overlaid is shown in Fig. 1. Figures 2 and 3 show the Δm distributions and the fit for each of the four categories and the two slow-pion charges. Table 2 lists the yields from the nominal fits and the resulting asymmetries. To obtain the final result, the asymmetries of the four signal categories are combined by taking the weighted mean.

5 Systematic uncertainties

The main sources of systematic effects are due to production and detection asymmetries and possible biases in the signal extraction method. The systematic uncertainty related to the signal extraction is estimated by comparing the nominal fit with an alternative one, where outside of the signal region of ± 1.5 MeV around the known Δm -value, only the background component is fitted. The signal yield is obtained by subtracting the background extrapolated into the signal region from the total observed yield. For the

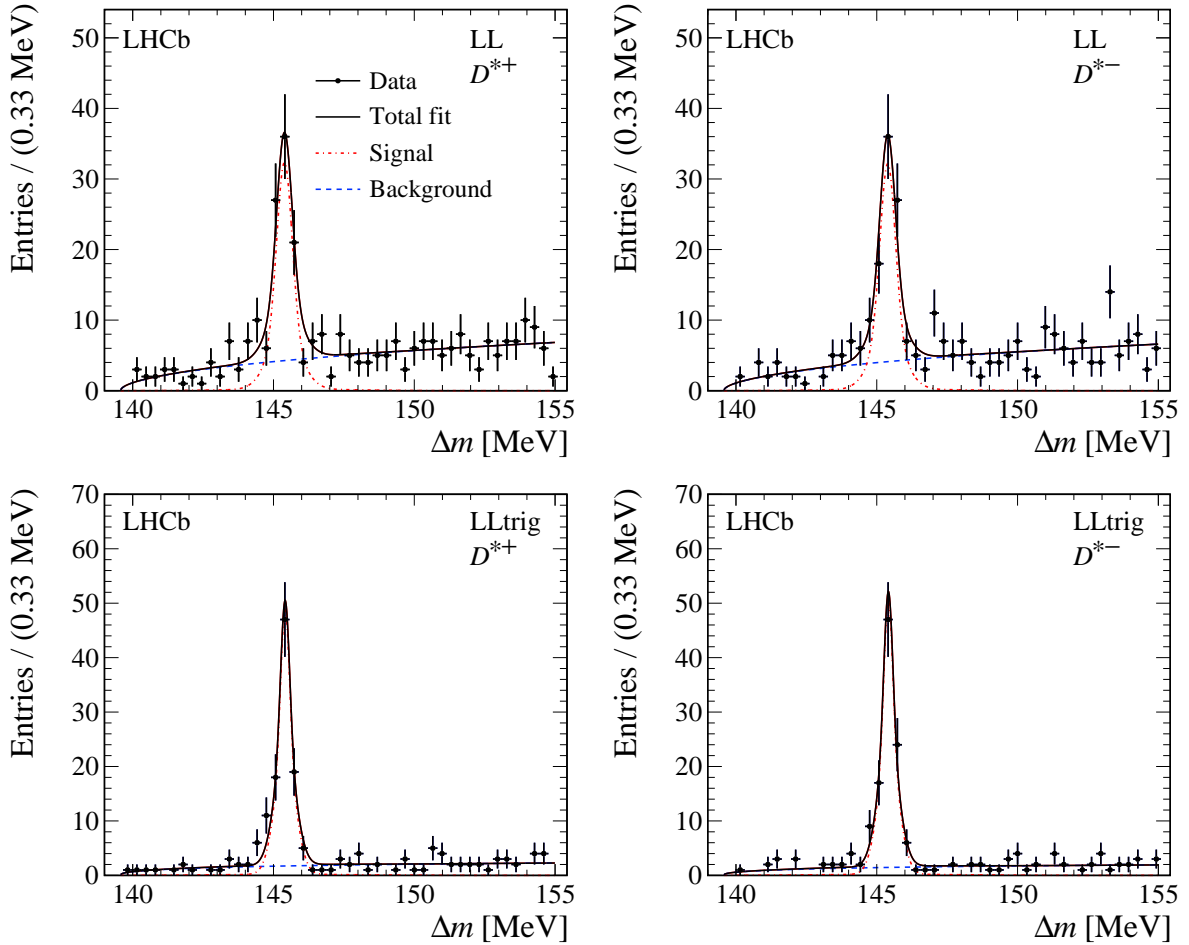


Figure 2: Distributions of Δm split into (left) D^{*+} , (right) D^{*-} and (top) LL, (bottom) LLtrig, including the fit function. The solid (black) line corresponds to the total fit, the dashed (blue) line corresponds to the background, and the dash-dotted (red) line represents the signal contribution.

combined CP asymmetry a difference of 0.019 is found, which is assigned as a systematic uncertainty.

The systematic effects that arise due to the slow pion charge asymmetry in the detector and a possible charge asymmetry of D^* production in pp collisions in the LHCb acceptance are determined using the control channel. However, the control channel contains charged kaons which introduce an additional detection asymmetry, as the interaction cross-sections of K^+ and K^- with the detector material are different. In Ref. [24], the charged kaon detection asymmetry has been measured to be in the range 0.008 to 0.012. Assuming the pion detection asymmetry to be negligible, and including possible trigger effects, a correction of -0.010 ± 0.005 is applied to the observed asymmetry in the control channel, resulting in a corrected value of -0.009 ± 0.005 . The absolute value of this number and its uncertainty are added in quadrature and assigned as a conservative estimate of the

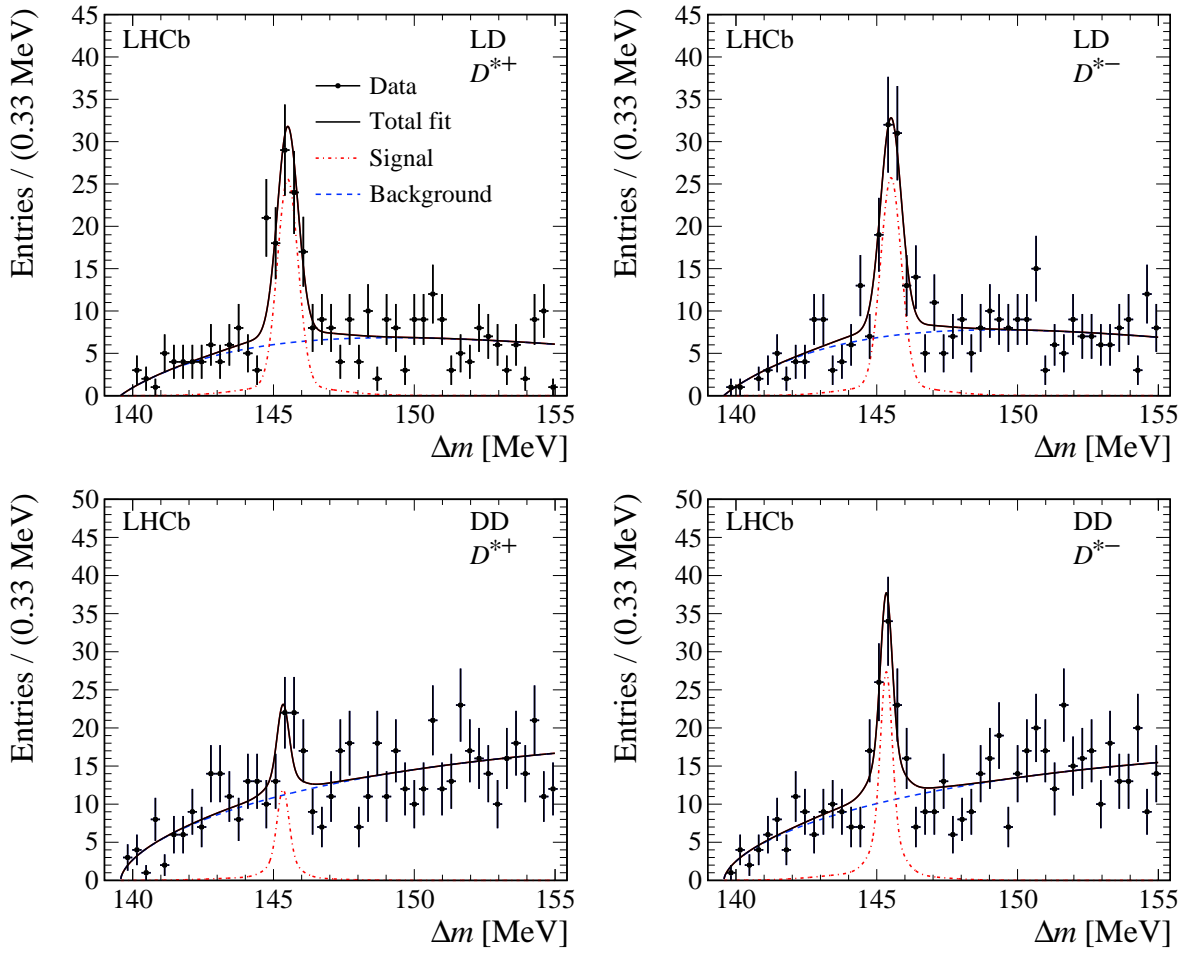


Figure 3: Distributions of Δm split into (left) D^{*+} , (right) D^{*-} and (top) LD, (bottom) DD, including the fit function. The solid (black) line corresponds to the total fit, the dashed (blue) line corresponds to the background, while the dash-dotted (red) line represents the signal contribution.

systematic uncertainty due to production and detection asymmetries.

Other checks have been performed but found to have statistically insignificant effects. These tests include the split into different trigger types, different run periods, and different magnet polarities. Also the effect of a possible difference in contamination by charm from beauty decays between signal and the control channel has been checked and found to be negligible. The total systematic uncertainty is calculated from the quadratic sum of the two dominant contributions, which come from the signal extraction (0.019) and the detection and production asymmetry (0.011), giving 0.022 for the total.

Table 2: Number of signal candidates and CP asymmetry obtained from the fits in the four categories.

Category	N^+	N^-	\mathcal{A}_{CP}
LL	86 ± 11	86 ± 12	0.00 ± 0.09
LD	82 ± 14	83 ± 13	-0.00 ± 0.11
DD	29 ± 14	66 ± 14	-0.39 ± 0.23
LLtrig	96 ± 11	99 ± 11	-0.02 ± 0.08
combined			-0.029 ± 0.052

6 Result

The time-integrated CP asymmetry in the decay $D^0 \rightarrow K_s^0 K_s^0$ is determined to be

$$\mathcal{A}_{CP} = -0.029 \pm 0.052 \pm 0.022 ,$$

where the first uncertainty is statistical and the second systematic. The result is consistent with no CP violation and with Standard Model expectations [7]. This is the single best measurement of this quantity to date, with an uncertainty more than three times smaller than the previous determination [8].

Acknowledgements

We express our gratitude to our colleagues in the CERN accelerator departments for the excellent performance of the LHC. We thank the technical and administrative staff at the LHCb institutes. We acknowledge support from CERN and from the national agencies: CAPES, CNPq, FAPERJ and FINEP (Brazil); NSFC (China); CNRS/IN2P3 (France); BMBF, DFG, HGF and MPG (Germany); INFN (Italy); FOM and NWO (The Netherlands); MNiSW and NCN (Poland); MEN/IFA (Romania); MinES and FANO (Russia); MinECo (Spain); SNSF and SER (Switzerland); NASU (Ukraine); STFC (United Kingdom); NSF (USA). The Tier1 computing centres are supported by IN2P3 (France), KIT and BMBF (Germany), INFN (Italy), NWO and SURF (The Netherlands), PIC (Spain), GridPP (United Kingdom). We are indebted to the communities behind the multiple open source software packages on which we depend. We are also thankful for the computing resources and the access to software R&D tools provided by Yandex LLC (Russia). Individual groups or members have received support from EPLANET, Marie Skłodowska-Curie Actions and ERC (European Union), Conseil général de Haute-Savoie, Labex ENIGMASS and OCEVU, Région Auvergne (France), RFBR (Russia), XuntaGal and GENCAT (Spain), Royal Society and Royal Commission for the Exhibition of 1851 (United Kingdom).

References

- [1] BaBar collaboration, B. Aubert *et al.*, *Search for CP violation in the decays $D^0 \rightarrow K^-K^+$ and $D^0 \rightarrow \pi^-\pi^+$* , Phys. Rev. Lett. **100** (2008) 061803, [arXiv:0709.2715](#).
- [2] CDF collaboration, T. Aaltonen *et al.*, *Measurement of the difference of CP-violating asymmetries in $D^0 \rightarrow K^+K^-$ and $D^0 \rightarrow \pi^+\pi^-$ decays at CDF*, Phys. Rev. Lett. **109** (2012) 111801, [arXiv:1207.2158](#).
- [3] B. R. Ko, *Direct CP violation in charm at Belle*, PoS **ICHEP2012** (2013) 353, [arXiv:1212.1975](#).
- [4] LHCb collaboration, *A search for time-integrated CP violation in $D^0 \rightarrow K^-K^+$ and $D^0 \rightarrow \pi^-\pi^+$ decays*, LHCb-CONF-2013-003.
- [5] LHCb collaboration, R. Aaij *et al.*, *Measurement of CP asymmetry in $D^0 \rightarrow K^-K^+$ and $D^0 \rightarrow \pi^-\pi^+$ decays*, JHEP **07** (2014) 041, [arXiv:1405.2797](#).
- [6] G. Hiller, M. Jung, S. Schacht, *SU(3)-flavor anatomy of nonleptonic charm decays*, Phys. Rev. **D87** (2013) 014024, [arXiv:1211.3734](#).
- [7] U. Nierste and S. Schacht, *CP violation in $D^0 \rightarrow K_s^0 K_s^0$* , Phys. Rev. **D92** (2015) 054036, [arXiv:1508.00074](#).
- [8] CLEO collaboration, G. Bonvicini *et al.*, *Search for CP violation in $D^0 \rightarrow K_s^0\pi^0$, $D^0 \rightarrow \pi^0\pi^0$ and $D^0 \rightarrow K_s^0K_s^0$ decays*, Phys. Rev. **D63** (2001) 071101(R), [arXiv:hep-ex/0012054](#).
- [9] LHCb collaboration, A. A. Alves Jr. *et al.*, *The LHCb detector at the LHC*, JINST **3** (2008) S08005.
- [10] LHCb collaboration, R. Aaij *et al.*, *LHCb detector performance*, Int. J. Mod. Phys. **A30** (2015) 1530022, [arXiv:1412.6352](#).
- [11] T. Sjöstrand, S. Mrenna, and P. Skands, *PYTHIA 6.4 physics and manual*, JHEP **05** (2006) 026, [arXiv:hep-ph/0603175](#); T. Sjöstrand, S. Mrenna, and P. Skands, *A brief introduction to PYTHIA 8.1*, Comput. Phys. Commun. **178** (2008) 852, [arXiv:0710.3820](#).
- [12] I. Belyaev *et al.*, *Handling of the generation of primary events in Gauss, the LHCb simulation framework*, J. Phys. Conf. Ser. **331** (2011) 032047.
- [13] D. J. Lange, *The EvtGen particle decay simulation package*, Nucl. Instrum. Meth. **A462** (2001) 152.
- [14] P. Golonka and Z. Was, *PHOTOS Monte Carlo: A precision tool for QED corrections in Z and W decays*, Eur. Phys. J. **C45** (2006) 97, [arXiv:hep-ph/0506026](#).

- [15] Geant4 collaboration, J. Allison *et al.*, *Geant4 developments and applications*, IEEE Trans. Nucl. Sci. **53** (2006) 270; Geant4 collaboration, S. Agostinelli *et al.*, *Geant4: A simulation toolkit*, Nucl. Instrum. Meth. **A506** (2003) 250.
- [16] M. Clemencic *et al.*, *The LHCb simulation application, Gauss: Design, evolution and experience*, J. Phys. Conf. Ser. **331** (2011) 032023.
- [17] W. D. Hulsbergen, *Decay chain fitting with a Kalman filter*, Nucl. Instrum. Meth. **A552** (2005) 566, [arXiv:physics/0503191](https://arxiv.org/abs/physics/0503191).
- [18] Particle Data Group, K. A. Olive *et al.*, *Review of particle physics*, Chin. Phys. **C38** (2014) 090001.
- [19] M. Britsch, N. Gagunashvili, and M. Schmelling, *Application of the rule-growing algorithm RIPPER to particle physics analysis*, PoS **ACAT08** (2008) 086, [arXiv:0910.1729](https://arxiv.org/abs/0910.1729).
- [20] M. Britsch, N. Gagunashvili, and M. Schmelling, *Classifying extremely imbalanced data sets*, PoS **ACAT2010** (2010) 047, [arXiv:1011.6224](https://arxiv.org/abs/1011.6224).
- [21] L. Breiman, *Bagging predictors*, Machine Learning **24** (1996) 123.
- [22] K. M. Ting, *An instance-weighting method to induce cost-sensitive trees*, IEEE Trans. Knowl. Data Eng. **14** (2002) 659.
- [23] H. Zhao, *Instance weighting versus threshold adjusting for cost-sensitive classification*, Knowl. Inf. Syst. **15** (2008) 321.
- [24] LHCb collaboration, R. Aaij *et al.*, *Measurement of D^0 - \bar{D}^0 mixing parameters and search for CP violation using $D^0 \rightarrow K^+\pi^-$ decays*, Phys. Rev. Lett. **111** (2013) 251801, [arXiv:1309.6534](https://arxiv.org/abs/1309.6534).

LHCb collaboration

R. Aaij³⁸, B. Adeva³⁷, M. Adinolfi⁴⁶, A. Affolder⁵², Z. Ajaltouni⁵, S. Akar⁶, J. Albrecht⁹, F. Alessio³⁸, M. Alexander⁵¹, S. Ali⁴¹, G. Alkhazov³⁰, P. Alvarez Cartelle⁵³, A.A. Alves Jr⁵⁷, S. Amato², S. Amerio²², Y. Amhis⁷, L. An³, L. Anderlini¹⁷, J. Anderson⁴⁰, G. Andreassi³⁹, M. Andreotti^{16,f}, J.E. Andrews⁵⁸, R.B. Appleby⁵⁴, O. Aquines Gutierrez¹⁰, F. Archilli³⁸, P. d'Argent¹¹, A. Artamonov³⁵, M. Artuso⁵⁹, E. Aslanides⁶, G. Auriemma^{25,m}, M. Baalouch⁵, S. Bachmann¹¹, J.J. Back⁴⁸, A. Badalov³⁶, C. Baesso⁶⁰, W. Baldini^{16,38}, R.J. Barlow⁵⁴, C. Barschel³⁸, S. Barsuk⁷, W. Barter³⁸, V. Batozskaya²⁸, V. Battista³⁹, A. Bay³⁹, L. Beaucourt⁴, J. Beddow⁵¹, F. Bedeschi²³, I. Bediaga¹, L.J. Bel⁴¹, V. Bellee³⁹, N. Belloli²⁰, I. Belyaev³¹, E. Ben-Haim⁸, G. Bencivenni¹⁸, S. Benson³⁸, J. Benton⁴⁶, A. Berezhnoy³², R. Bernet⁴⁰, A. Bertolin²², M.-O. Bettler³⁸, M. van Beuzekom⁴¹, A. Bien¹¹, S. Bifani⁴⁵, P. Billoir⁸, T. Bird⁵⁴, A. Birnkraut⁹, A. Bizzeti^{17,h}, T. Blake⁴⁸, F. Blanc³⁹, J. Blouw¹⁰, S. Blusk⁵⁹, V. Bocci²⁵, A. Bondar³⁴, N. Bondar^{30,38}, W. Bonivento¹⁵, S. Borghi⁵⁴, M. Borsato⁷, T.J.V. Bowcock⁵², E. Bowen⁴⁰, C. Bozzi¹⁶, S. Braun¹¹, M. Britsch¹⁰, T. Britton⁵⁹, J. Brodzicka⁵⁴, N.H. Brook⁴⁶, E. Buchanan⁴⁶, A. Bursche⁴⁰, J. Buytaert³⁸, S. Cadeddu¹⁵, R. Calabrese^{16,f}, M. Calvi^{20,j}, M. Calvo Gomez^{36,o}, P. Campana¹⁸, D. Campora Perez³⁸, L. Capriotti⁵⁴, A. Carbone^{14,d}, G. Carboni^{24,k}, R. Cardinale^{19,i}, A. Cardini¹⁵, P. Carniti²⁰, L. Carson⁵⁰, K. Carvalho Akiba^{2,38}, G. Casse⁵², L. Cassina^{20,j}, L. Castillo Garcia³⁸, M. Cattaneo³⁸, Ch. Cauet⁹, G. Cavallero¹⁹, R. Cenci^{23,s}, M. Charles⁸, Ph. Charpentier³⁸, M. Chefdeville⁴, S. Chen⁵⁴, S.-F. Cheung⁵⁵, N. Chiapolini⁴⁰, M. Chrzaszcz⁴⁰, X. Cid Vidal³⁸, G. Ciezarek⁴¹, P.E.L. Clarke⁵⁰, M. Clemencic³⁸, H.V. Cliff⁴⁷, J. Closier³⁸, V. Coco³⁸, J. Cogan⁶, E. Cogneras⁵, V. Cogoni^{15,e}, L. Cojocariu²⁹, G. Collazuol²², P. Collins³⁸, A. Comerma-Montells¹¹, A. Contu^{15,38}, A. Cook⁴⁶, M. Coombes⁴⁶, S. Coquereau⁸, G. Corti³⁸, M. Corvo^{16,f}, B. Couturier³⁸, G.A. Cowan⁵⁰, D.C. Craik⁴⁸, A. Crocombe⁴⁸, M. Cruz Torres⁶⁰, S. Cunliffe⁵³, R. Currie⁵³, C. D'Ambrosio³⁸, E. Dall'Occo⁴¹, J. Dalseno⁴⁶, P.N.Y. David⁴¹, A. Davis⁵⁷, K. De Bruyn⁴¹, S. De Capua⁵⁴, M. De Cian¹¹, J.M. De Miranda¹, L. De Paula², P. De Simone¹⁸, C.-T. Dean⁵¹, D. Decamp⁴, M. Deckenhoff⁹, L. Del Buono⁸, N. Déléage⁴, M. Demmer⁹, D. Derkach⁵⁵, O. Deschamps⁵, F. Dettori³⁸, B. Dey²¹, A. Di Canto³⁸, F. Di Ruscio²⁴, H. Dijkstra³⁸, S. Donleavy⁵², F. Dordei¹¹, M. Dorigo³⁹, A. Dosil Suárez³⁷, D. Dossett⁴⁸, A. Dovbnya⁴³, K. Dreimanis⁵², L. Dufour⁴¹, G. Dujany⁵⁴, F. Dupertuis³⁹, P. Durante³⁸, R. Dzhelyadin³⁵, A. Dziurda²⁶, A. Dzyuba³⁰, S. Easo^{49,38}, U. Egede⁵³, V. Egorychev³¹, S. Eidelman³⁴, S. Eisenhardt⁵⁰, U. Eitschberger⁹, R. Ekelhof⁹, L. Eklund⁵¹, I. El Rifai⁵, Ch. Elsasser⁴⁰, S. Ely⁵⁹, S. Esen¹¹, H.M. Evans⁴⁷, T. Evans⁵⁵, A. Falabella¹⁴, C. Färber³⁸, N. Farley⁴⁵, S. Farry⁵², R. Fay⁵², D. Ferguson⁵⁰, V. Fernandez Albor³⁷, F. Ferrari¹⁴, F. Ferreira Rodrigues¹, M. Ferro-Luzzi³⁸, S. Filippov³³, M. Fiore^{16,38,f}, M. Fiorini^{16,f}, M. Firlej²⁷, C. Fitzpatrick³⁹, T. Fiutowski²⁷, K. Fohl³⁸, P. Fol⁵³, M. Fontana¹⁵, F. Fontanelli^{19,i}, R. Forty³⁸, O. Francisco², M. Frank³⁸, C. Frei³⁸, M. Frosini¹⁷, J. Fu²¹, E. Furfarò^{24,k}, A. Gallas Torreira³⁷, D. Galli^{14,d}, S. Gallorini^{22,38}, S. Gambetta⁵⁰, M. Gandelman², P. Gandini⁵⁵, Y. Gao³, J. García Pardiñas³⁷, J. Garra Tico⁴⁷, L. Garrido³⁶, D. Gascon³⁶, C. Gaspar³⁸, R. Gauld⁵⁵, L. Gavardi⁹, G. Gazzoni⁵, D. Gerick¹¹, E. Gersabeck¹¹, M. Gersabeck⁵⁴, T. Gershon⁴⁸, Ph. Ghez⁴, S. Giani³⁹, V. Gibson⁴⁷, O. G. Girard³⁹, L. Giubega²⁹, V.V. Gligorov³⁸, C. Göbel⁶⁰, D. Golubkov³¹, A. Golutvin^{53,31,38}, A. Gomes^{1,a}, C. Gotti^{20,j}, M. Grabalosa Gándara⁵, R. Graciani Diaz³⁶, L.A. Granado Cardoso³⁸, E. Graugés³⁶, E. Graverini⁴⁰, G. Graziani¹⁷, A. Grecu²⁹, E. Greening⁵⁵, S. Gregson⁴⁷, P. Griffith⁴⁵, L. Grillo¹¹, O. Grünberg⁶³, B. Gui⁵⁹, E. Gushchin³³, Yu. Guz^{35,38}, T. Gys³⁸, T. Hadavizadeh⁵⁵, C. Hadjivasiliou⁵⁹, G. Haefeli³⁹, C. Haen³⁸, S.C. Haines⁴⁷, S. Hall⁵³,

B. Hamilton⁵⁸, X. Han¹¹, S. Hansmann-Menzemer¹¹, N. Harnew⁵⁵, S.T. Harnew⁴⁶, J. Harrison⁵⁴, J. He³⁸, T. Head³⁹, V. Heijne⁴¹, K. Hennessy⁵², P. Henrard⁵, L. Henry⁸, E. van Herwijnen³⁸, M. Heß⁶³, A. Hicheur², D. Hill⁵⁵, M. Hoballah⁵, C. Hombach⁵⁴, W. Hulsbergen⁴¹, T. Humair⁵³, N. Hussain⁵⁵, D. Hutchcroft⁵², D. Hynds⁵¹, M. Idzik²⁷, P. Ilten⁵⁶, R. Jacobsson³⁸, A. Jaeger¹¹, J. Jalocha⁵⁵, E. Jans⁴¹, A. Jawahery⁵⁸, F. Jing³, M. John⁵⁵, D. Johnson³⁸, C.R. Jones⁴⁷, C. Joram³⁸, B. Jost³⁸, N. Jurik⁵⁹, S. Kandybei⁴³, W. Kango⁶, M. Karacson³⁸, T.M. Karbach^{38,†}, S. Karodia⁵¹, M. Kecke¹¹, M. Kelsey⁵⁹, I.R. Kenyon⁴⁵, M. Kenzie³⁸, T. Ketel⁴², B. Khanji^{20,38,j}, C. Khurewathanakul³⁹, S. Klaver⁵⁴, K. Klimaszewski²⁸, O. Kochebina⁷, M. Kolpin¹¹, I. Komarov³⁹, R.F. Koopman⁴², P. Koppenburg^{41,38}, M. Kozeiha⁵, L. Kravchuk³³, K. Kreplin¹¹, M. Kreps⁴⁸, G. Krocker¹¹, P. Krokovny³⁴, F. Kruse⁹, W. Krzemien²⁸, W. Kucewicz^{26,n}, M. Kucharczyk²⁶, V. Kudryavtsev³⁴, A. K. Kuonen³⁹, K. Kurek²⁸, T. Kvaratskheliya³¹, D. Lacarrere³⁸, G. Lafferty⁵⁴, A. Lai¹⁵, D. Lambert⁵⁰, G. Lanfranchi¹⁸, C. Langenbruch⁴⁸, B. Langhans³⁸, T. Latham⁴⁸, C. Lazzeroni⁴⁵, R. Le Gac⁶, J. van Leerdam⁴¹, J.-P. Lees⁴, R. Lefèvre⁵, A. Leflat^{32,38}, J. Lefrançois⁷, O. Leroy⁶, T. Lesiak²⁶, B. Leverington¹¹, Y. Li⁷, T. Likhomanenko^{65,64}, M. Liles⁵², R. Lindner³⁸, C. Linn³⁸, F. Lionetto⁴⁰, B. Liu¹⁵, X. Liu³, D. Loh⁴⁸, I. Longstaff⁵¹, J.H. Lopes², D. Lucchesi^{22,q}, M. Lucio Martinez³⁷, H. Luo⁵⁰, A. Lupato²², E. Luppi^{16,f}, O. Lupton⁵⁵, A. Lusiani²³, F. Machefert⁷, F. Maciuc²⁹, O. Maev³⁰, K. Maguire⁵⁴, S. Malde⁵⁵, A. Malinin⁶⁴, G. Manca⁷, G. Mancinelli⁶, P. Manning⁵⁹, A. Mapelli³⁸, J. Maratas⁵, J.F. Marchand⁴, U. Marconi¹⁴, C. Marin Benito³⁶, P. Marino^{23,38,s}, J. Marks¹¹, G. Martellotti²⁵, M. Martin⁶, M. Martinelli³⁹, D. Martinez Santos³⁷, F. Martinez Vidal⁶⁶, D. Martins Tostes², A. Massafferri¹, R. Matev³⁸, A. Mathad⁴⁸, Z. Mathe³⁸, C. Matteuzzi²⁰, A. Mauri⁴⁰, B. Maurin³⁹, A. Mazurov⁴⁵, M. McCann⁵³, J. McCarthy⁴⁵, A. McNab⁵⁴, R. McNulty¹², B. Meadows⁵⁷, F. Meier⁹, M. Meissner¹¹, D. Melnychuk²⁸, M. Merk⁴¹, E Michielin²², D.A. Milanes⁶², M.-N. Minard⁴, D.S. Mitzel¹¹, J. Molina Rodriguez⁶⁰, I.A. Monroy⁶², S. Monteil⁵, M. Morandin²², P. Morawski²⁷, A. Mordà⁶, M.J. Morello^{23,s}, J. Moron²⁷, A.B. Morris⁵⁰, R. Mountain⁵⁹, F. Muheim⁵⁰, D. Müller⁵⁴, J. Müller⁹, K. Müller⁴⁰, V. Müller⁹, M. Mussini¹⁴, B. Muster³⁹, P. Naik⁴⁶, T. Nakada³⁹, R. Nandakumar⁴⁹, A. Nandi⁵⁵, I. Nasteva², M. Needham⁵⁰, N. Neri²¹, S. Neubert¹¹, N. Neufeld³⁸, M. Neuner¹¹, A.D. Nguyen³⁹, T.D. Nguyen³⁹, C. Nguyen-Mau^{39,p}, V. Niess⁵, R. Niet⁹, N. Nikitin³², T. Nikodem¹¹, D. Ninci²³, A. Novoselov³⁵, D.P. O'Hanlon⁴⁸, A. Oblakowska-Mucha²⁷, V. Obraztsov³⁵, S. Ogilvy⁵¹, O. Okhrimenko⁴⁴, R. Oldeman^{15,e}, C.J.G. Onderwater⁶⁷, B. Osorio Rodrigues¹, J.M. Otalora Goicochea², A. Otto³⁸, P. Owen⁵³, A. Oyanguren⁶⁶, A. Palano^{13,c}, F. Palombo^{21,t}, M. Palutan¹⁸, J. Panman³⁸, A. Papanestis⁴⁹, M. Pappagallo⁵¹, L.L. Pappalardo^{16,f}, C. Pappenheimer⁵⁷, C. Parkes⁵⁴, G. Passaleva¹⁷, G.D. Patel⁵², M. Patel⁵³, C. Patrignani^{19,i}, A. Pearce^{54,49}, A. Pellegrino⁴¹, G. Penso^{25,l}, M. Pepe Altarelli³⁸, S. Perazzini^{14,d}, P. Perret⁵, L. Pescatore⁴⁵, K. Petridis⁴⁶, A. Petrolini^{19,i}, M. Petruzzo²¹, E. Picatoste Olloqui³⁶, B. Pietrzyk⁴, T. Pilar⁴⁸, D. Pinci²⁵, A. Pistone¹⁹, A. Piucci¹¹, S. Playfer⁵⁰, M. Plo Casasus³⁷, T. Poikela³⁸, F. Polci⁸, A. Poluektov^{48,34}, I. Polyakov³¹, E. Polycarpo², A. Popov³⁵, D. Popov^{10,38}, B. Popovici²⁹, C. Potterat², E. Price⁴⁶, J.D. Price⁵², J. Prisciandaro³⁹, A. Pritchard⁵², C. Prouve⁴⁶, V. Pugatch⁴⁴, A. Puig Navarro³⁹, G. Punzi^{23,r}, W. Qian⁴, R. Quagliani^{7,46}, B. Rachwal²⁶, J.H. Rademacker⁴⁶, M. Rama²³, M.S. Rangel², I. Raniuk⁴³, N. Rauschmayr³⁸, G. Raven⁴², F. Redi⁵³, S. Reichert⁵⁴, M.M. Reid⁴⁸, A.C. dos Reis¹, S. Ricciardi⁴⁹, S. Richards⁴⁶, M. Rihl³⁸, K. Rinnert⁵², V. Rives Molina³⁶, P. Robbe^{7,38}, A.B. Rodrigues¹, E. Rodrigues⁵⁴, J.A. Rodriguez Lopez⁶², P. Rodriguez Perez⁵⁴, S. Roiser³⁸, V. Romanovsky³⁵, A. Romero Vidal³⁷, J. W. Ronayne¹², M. Rotondo²², J. Rouvinet³⁹, T. Ruf³⁸, P. Ruiz Valls⁶⁶, J.J. Saborido Silva³⁷, N. Sagidova³⁰, P. Sail⁵¹, B. Saitta^{15,e},

V. Salustino Guimaraes², C. Sanchez Mayordomo⁶⁶, B. Sanmartin Sedes³⁷, R. Santacesaria²⁵,
 C. Santamarina Rios³⁷, M. Santimaria¹⁸, E. Santovetti^{24,k}, A. Sarti^{18,l}, C. Satriano^{25,m},
 A. Satta²⁴, D.M. Saunders⁴⁶, D. Savrina^{31,32}, M. Schiller³⁸, H. Schindler³⁸, M. Schlupp⁹,
 M. Schmelling¹⁰, T. Schmelzer⁹, B. Schmidt³⁸, O. Schneider³⁹, A. Schopper³⁸, M. Schubiger³⁹,
 M.-H. Schune⁷, R. Schwemmer³⁸, B. Sciascia¹⁸, A. Sciubba^{25,l}, A. Semennikov³¹, N. Serra⁴⁰,
 J. Serrano⁶, L. Sestini²², P. Seyfert²⁰, M. Shapkin³⁵, I. Shapoval^{16,43,f}, Y. Shcheglov³⁰,
 T. Shears⁵², L. Shekhtman³⁴, V. Shevchenko⁶⁴, A. Shires⁹, B.G. Siddi¹⁶, R. Silva Coutinho^{48,40},
 L. Silva de Oliveira², G. Simi²², M. Sirendi⁴⁷, N. Skidmore⁴⁶, I. Skillicorn⁵¹, T. Skwarnicki⁵⁹,
 E. Smith^{55,49}, E. Smith⁵³, I. T. Smith⁵⁰, J. Smith⁴⁷, M. Smith⁵⁴, H. Snoek⁴¹, M.D. Sokoloff^{57,38},
 F.J.P. Soler⁵¹, F. Soomro³⁹, D. Souza⁴⁶, B. Souza De Paula², B. Spaan⁹, P. Spradlin⁵¹,
 S. Sridharan³⁸, F. Stagni³⁸, M. Stahl¹¹, S. Stahl³⁸, S. Stefkova⁵³, O. Steinkamp⁴⁰,
 O. Stenyakin³⁵, S. Stevenson⁵⁵, S. Stoica²⁹, S. Stone⁵⁹, B. Storaci⁴⁰, S. Stracka^{23,s},
 M. Stratificiu²⁹, U. Straumann⁴⁰, L. Sun⁵⁷, W. Sutcliffe⁵³, K. Swientek²⁷, S. Swientek⁹,
 V. Syropoulos⁴², M. Szczekowski²⁸, P. Szczypka^{39,38}, T. Szumlak²⁷, S. T'Jampens⁴,
 A. Tayduganov⁶, T. Tekampe⁹, M. Teklishyn⁷, G. Tellarini^{16,f}, F. Teubert³⁸, C. Thomas⁵⁵,
 E. Thomas³⁸, J. van Tilburg⁴¹, V. Tisserand⁴, M. Tobin³⁹, J. Todd⁵⁷, S. Tolk⁴²,
 L. Tomassetti^{16,f}, D. Tonelli³⁸, S. Topp-Joergensen⁵⁵, N. Torr⁵⁵, E. Tournefier⁴, S. Tourneur³⁹,
 K. Trabelsi³⁹, M.T. Tran³⁹, M. Tresch⁴⁰, A. Trisovic³⁸, A. Tsaregorodtsev⁶, P. Tsopelas⁴¹,
 N. Tuning^{41,38}, A. Ukleja²⁸, A. Ustyuzhanin^{65,64}, U. Uwer¹¹, C. Vacca^{15,e}, V. Vagnoni¹⁴,
 G. Valenti¹⁴, A. Vallier⁷, R. Vazquez Gomez¹⁸, P. Vazquez Regueiro³⁷, C. Vázquez Sierra³⁷,
 S. Vecchi¹⁶, J.J. Velthuis⁴⁶, M. Velttri^{17,g}, G. Veneziano³⁹, M. Vesterinen¹¹, B. Viaud⁷,
 D. Vieira², M. Vieites Diaz³⁷, X. Vilasis-Cardona^{36,o}, V. Volkov³², A. Vollhardt⁴⁰,
 D. Volyansky¹⁰, D. Voong⁴⁶, A. Vorobyev³⁰, V. Vorobyev³⁴, C. Voß⁶³, J.A. de Vries⁴¹,
 R. Waldi⁶³, C. Wallace⁴⁸, R. Wallace¹², J. Walsh²³, S. Wandernoth¹¹, J. Wang⁵⁹, D.R. Ward⁴⁷,
 N.K. Watson⁴⁵, D. Websdale⁵³, A. Weiden⁴⁰, M. Whitehead⁴⁸, G. Wilkinson^{55,38},
 M. Wilkinson⁵⁹, M. Williams³⁸, M.P. Williams⁴⁵, M. Williams⁵⁶, T. Williams⁴⁵, F.F. Wilson⁴⁹,
 J. Wimberley⁵⁸, J. Wishahi⁹, W. Wislicki²⁸, M. Witek²⁶, G. Wormser⁷, S.A. Wotton⁴⁷,
 S. Wright⁴⁷, K. Wyllie³⁸, Y. Xie⁶¹, Z. Xu³⁹, Z. Yang³, J. Yu⁶¹, X. Yuan³⁴, O. Yushchenko³⁵,
 M. Zangoli¹⁴, M. Zavertyaev^{10,b}, L. Zhang³, Y. Zhang³, A. Zhelezov¹¹, A. Zhokhov³¹, L. Zhong³,
 S. Zucchelli¹⁴.

¹Centro Brasileiro de Pesquisas Físicas (CBPF), Rio de Janeiro, Brazil

²Universidade Federal do Rio de Janeiro (UFRJ), Rio de Janeiro, Brazil

³Center for High Energy Physics, Tsinghua University, Beijing, China

⁴LAPP, Université Savoie Mont-Blanc, CNRS/IN2P3, Annecy-Le-Vieux, France

⁵Clermont Université, Université Blaise Pascal, CNRS/IN2P3, LPC, Clermont-Ferrand, France

⁶CPPM, Aix-Marseille Université, CNRS/IN2P3, Marseille, France

⁷LAL, Université Paris-Sud, CNRS/IN2P3, Orsay, France

⁸LPNHE, Université Pierre et Marie Curie, Université Paris Diderot, CNRS/IN2P3, Paris, France

⁹Fakultät Physik, Technische Universität Dortmund, Dortmund, Germany

¹⁰Max-Planck-Institut für Kernphysik (MPIK), Heidelberg, Germany

¹¹Physikalisches Institut, Ruprecht-Karls-Universität Heidelberg, Heidelberg, Germany

¹²School of Physics, University College Dublin, Dublin, Ireland

¹³Sezione INFN di Bari, Bari, Italy

¹⁴Sezione INFN di Bologna, Bologna, Italy

¹⁵Sezione INFN di Cagliari, Cagliari, Italy

¹⁶Sezione INFN di Ferrara, Ferrara, Italy

¹⁷Sezione INFN di Firenze, Firenze, Italy

- ¹⁸*Laboratori Nazionali dell'INFN di Frascati, Frascati, Italy*
- ¹⁹*Sezione INFN di Genova, Genova, Italy*
- ²⁰*Sezione INFN di Milano Bicocca, Milano, Italy*
- ²¹*Sezione INFN di Milano, Milano, Italy*
- ²²*Sezione INFN di Padova, Padova, Italy*
- ²³*Sezione INFN di Pisa, Pisa, Italy*
- ²⁴*Sezione INFN di Roma Tor Vergata, Roma, Italy*
- ²⁵*Sezione INFN di Roma La Sapienza, Roma, Italy*
- ²⁶*Henryk Niewodniczanski Institute of Nuclear Physics Polish Academy of Sciences, Kraków, Poland*
- ²⁷*AGH - University of Science and Technology, Faculty of Physics and Applied Computer Science, Kraków, Poland*
- ²⁸*National Center for Nuclear Research (NCBJ), Warsaw, Poland*
- ²⁹*Horia Hulubei National Institute of Physics and Nuclear Engineering, Bucharest-Magurele, Romania*
- ³⁰*Petersburg Nuclear Physics Institute (PNPI), Gatchina, Russia*
- ³¹*Institute of Theoretical and Experimental Physics (ITEP), Moscow, Russia*
- ³²*Institute of Nuclear Physics, Moscow State University (SINP MSU), Moscow, Russia*
- ³³*Institute for Nuclear Research of the Russian Academy of Sciences (INR RAN), Moscow, Russia*
- ³⁴*Budker Institute of Nuclear Physics (SB RAS) and Novosibirsk State University, Novosibirsk, Russia*
- ³⁵*Institute for High Energy Physics (IHEP), Protvino, Russia*
- ³⁶*Universitat de Barcelona, Barcelona, Spain*
- ³⁷*Universidad de Santiago de Compostela, Santiago de Compostela, Spain*
- ³⁸*European Organization for Nuclear Research (CERN), Geneva, Switzerland*
- ³⁹*Ecole Polytechnique Fédérale de Lausanne (EPFL), Lausanne, Switzerland*
- ⁴⁰*Physik-Institut, Universität Zürich, Zürich, Switzerland*
- ⁴¹*Nikhef National Institute for Subatomic Physics, Amsterdam, The Netherlands*
- ⁴²*Nikhef National Institute for Subatomic Physics and VU University Amsterdam, Amsterdam, The Netherlands*
- ⁴³*NSC Kharkiv Institute of Physics and Technology (NSC KIPT), Kharkiv, Ukraine*
- ⁴⁴*Institute for Nuclear Research of the National Academy of Sciences (KINR), Kyiv, Ukraine*
- ⁴⁵*University of Birmingham, Birmingham, United Kingdom*
- ⁴⁶*H.H. Wills Physics Laboratory, University of Bristol, Bristol, United Kingdom*
- ⁴⁷*Cavendish Laboratory, University of Cambridge, Cambridge, United Kingdom*
- ⁴⁸*Department of Physics, University of Warwick, Coventry, United Kingdom*
- ⁴⁹*STFC Rutherford Appleton Laboratory, Didcot, United Kingdom*
- ⁵⁰*School of Physics and Astronomy, University of Edinburgh, Edinburgh, United Kingdom*
- ⁵¹*School of Physics and Astronomy, University of Glasgow, Glasgow, United Kingdom*
- ⁵²*Oliver Lodge Laboratory, University of Liverpool, Liverpool, United Kingdom*
- ⁵³*Imperial College London, London, United Kingdom*
- ⁵⁴*School of Physics and Astronomy, University of Manchester, Manchester, United Kingdom*
- ⁵⁵*Department of Physics, University of Oxford, Oxford, United Kingdom*
- ⁵⁶*Massachusetts Institute of Technology, Cambridge, MA, United States*
- ⁵⁷*University of Cincinnati, Cincinnati, OH, United States*
- ⁵⁸*University of Maryland, College Park, MD, United States*
- ⁵⁹*Syracuse University, Syracuse, NY, United States*
- ⁶⁰*Pontifícia Universidade Católica do Rio de Janeiro (PUC-Rio), Rio de Janeiro, Brazil, associated to ²*
- ⁶¹*Institute of Particle Physics, Central China Normal University, Wuhan, Hubei, China, associated to ³*
- ⁶²*Departamento de Fisica , Universidad Nacional de Colombia, Bogota, Colombia, associated to ⁸*
- ⁶³*Institut für Physik, Universität Rostock, Rostock, Germany, associated to ¹¹*
- ⁶⁴*National Research Centre Kurchatov Institute, Moscow, Russia, associated to ³¹*
- ⁶⁵*Yandex School of Data Analysis, Moscow, Russia, associated to ³¹*
- ⁶⁶*Instituto de Fisica Corpuscular (IFIC), Universitat de Valencia-CSIC, Valencia, Spain, associated to ³⁶*
- ⁶⁷*Van Swinderen Institute, University of Groningen, Groningen, The Netherlands, associated to ⁴¹*

- ^a Universidade Federal do Triângulo Mineiro (UFTM), Uberaba-MG, Brazil
^b P.N. Lebedev Physical Institute, Russian Academy of Science (LPI RAS), Moscow, Russia
^c Università di Bari, Bari, Italy
^d Università di Bologna, Bologna, Italy
^e Università di Cagliari, Cagliari, Italy
^f Università di Ferrara, Ferrara, Italy
^g Università di Urbino, Urbino, Italy
^h Università di Modena e Reggio Emilia, Modena, Italy
ⁱ Università di Genova, Genova, Italy
^j Università di Milano Bicocca, Milano, Italy
^k Università di Roma Tor Vergata, Roma, Italy
^l Università di Roma La Sapienza, Roma, Italy
^m Università della Basilicata, Potenza, Italy
ⁿ AGH - University of Science and Technology, Faculty of Computer Science, Electronics and Telecommunications, Kraków, Poland
^o LIFAELS, La Salle, Universitat Ramon Llull, Barcelona, Spain
^p Hanoi University of Science, Hanoi, Viet Nam
^q Università di Padova, Padova, Italy
^r Università di Pisa, Pisa, Italy
^s Scuola Normale Superiore, Pisa, Italy
^t Università degli Studi di Milano, Milano, Italy

† Deceased